ACOUSTIC MICROSCOPY WALL THICKNESS MEASUREMENTS ON NICKEL BASED SUPERALLOY GAS TURBINE BLADES

G. M. Amulele, A. G. Every,
Department of Physics, University of the Witwatersrand,
PO Wits 2050,
Johannesburg, South Africa.

S. C. Yates,
MATTEK, CSIR,
PO Box 395,
Pretoria 0001,
South Africa.

INTRODUCTION

In the manufacture of hollow jet engine turbine blades, monitoring the wall thickness is an important component of quality control. Because of the inaccessibility of the inner air channel to mechanical probing, ultrasonics provides one of the few means by which the necessary measurements can be done. The complex shape of the blades and the fact that they are often acoustically anisotropic make this a challenging problem. Alternative techniques have been investigated[1] for the wall thickness measurements but ultrasonics still presents the best option, and hence the continued interest in this problem[2].

In this paper we report on a procedure we have implemented on a laboratory scale for carrying out wall thickness measurements on hollow single crystal superalloy gas turbine blades. The particular superalloy used is nickel-based and is known as *SMP-2*; it is very similar in composition to *CMSX-4*. Our procedure is based on pulse echo time of flight measurements carried out in a water tank with a focused ultrasonic probe. By scanning the probe, the variation of the wall thickness over the blade is obtained. Prior to the ultrasonic measurements, the external profile of the blade is recorded with a coordinate measuring machine. Extraction of the wall thickness from time of flight data requires knowledge of the crystallographic orientation of the component so that the dependence of the ultrasound velocity on the direction can be determined. This is obtained by Laue X-ray diffraction.

EXPERIMENTAL DETAILS AND APPARATUS.

The procedure we have implemented comprises three steps. First, the component's external profile is determined using an *LK G80C* coordinate measuring machine (CMM) and recorded as a set of points in a 3-D Cartesian coordinate system. Then, using a

Review of Progress in Quantitative Nondestructive Evaluation, Vol. 18
Edited by Thompson and Chimenti, Kluwer Academic/Plenum Publishers, 1999

customized transmission Laue X-ray diffraction setup, the crystallographic orientation of the component is determined with respect to the component's axes defined by the CMM. The component's profile is then transferred, as a file, from the CMM's host computer to a computer interfaced with the scanning ultrasonic probe (*FATHOM IM90* Scanning Acoustic Microscope). The component profile data is used to control the movement of the scanning probe, keeping it normal to, and with focal point on the surface of the component. The ultrasonic probe is operated in pulsed mode and time of flight data pertaining to the front and back wall echoes is collected. The extraction of the wall thickness from this data is discussed in a later section.

A preliminary investigation was carried out on a specially cast test piece in the shape of a cylinder with a conical cap as depicted in figure 1. The shape of the test piece provided scope for ultrasonic measurements in a wide range of crystallographic directions. Since this shape and hence the wall thickness could be accurately measured with the CMM, the test component provided a way of confirming the crystallographic orientation measurement technique and also yielded an optimized set of elastic constants for the superalloy.

The inner concave and outer convex surfaces of the casting are labelled the high pressure (*hp*) and low pressure (*lp*) sides respectively, in conformity with the terminology for turbine blades. The computer interfaced to the SAM created a 'scan plan' which also comprised a set of direction cosines of normals at all the profile points using the *lp* file generated by the CMM. The ultrasonic probe, operating at 25MHz, used this data to align itself normally to the sample surface and with focal point on that surface as it scanned the component. For normal isonification the wavenormal remains unchanged as the ultrasonic pulse passes between the water transmission medium and the component, regardless of anisotropy. Also, since the wall thickness is much less than the radius of curvature of the component, the component can be regarded as locally flat, and the reflection off the opposite surface also involves no change in the wave normal. Under these conditions the transit time of the ultrasonic pulse in the solid is given simply in terms of the wall thickness and ultrasonic phase velocity υ_p in the direction normal to the

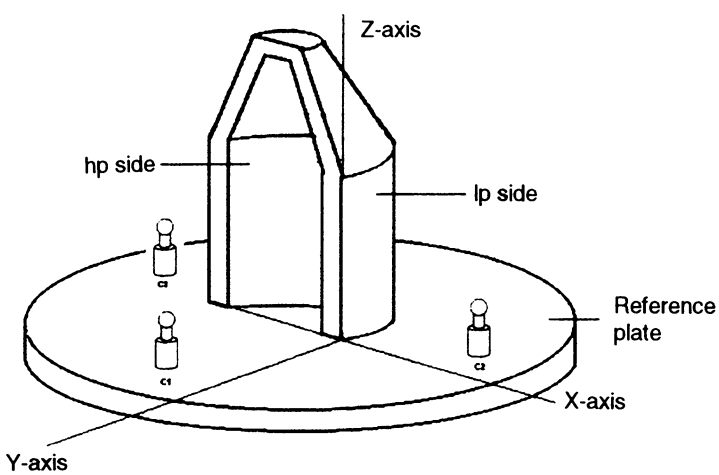

Figure 1: The test component. The centers of the three spheres C1, C2 and C3 attached to the reference plate are used by the CMM as reference points to define the component's axes system and as reference points by the SAM for its scanning operation.

component's surface. In our coding to calculate the directional dependence of the phase velocity we have made use of closed form solutions of Christoffel's equations[3]. The dominant echo that we observe corresponds to longitudinal (L) wave transmission through the component. In non-symmetry directions there is significant mode conversion and pronounced transverse (T) wave echoes can be observed. We comment on these in a later section. Using the L echo, the thickness d at each profile point was obtained from the transit time t measured there by

$$d = \frac{\upsilon_p(L)t}{2} \tag{1}$$

These ultrasonically measured thicknesses were then compared with the mechanically measured values. The latter were obtained by utilizing the CMM file for the *hp* side to generate a spline surface, from which the minimum distances to the *lp* profile points were taken as the actual thickness measurements.

The calculation of $\upsilon_p(L)$ requires knowledge of the three elastic constants C_{11}, C_{12}, and C_{44} of the superalloy. Data on these constants was available from two sources[4][5]. While reasonable agreement between the ultrasonically and mechanically measured thicknesses was obtained using these elastic constants, we found that the fit could be significantly improved by adjusting the values of the elastic constants. We obtained an optimum set of elastic constants by minimizing

$$\chi^2 = \sum_i (d_i^{ultra} - d_i^{meas})^2 \tag{2}$$

where the sum is over all the profile points at which thickness measurements were taken and runs over both the cylindrical and conical sections of the test piece, d_i^{meas} are the thicknesses measured by the CMM and d_i^{ultra} the ultrasonically determined thicknesses at the profile points.

RESULTS AND DISCUSSIONS

Table 1 shows the elastic constant values obtained in our fitting procedure for data on the test component together with the values obtained by a resonance technique[4] and by a pulse echo technique[5]. The density of the superalloy is 8.73g/cm^3.

Figure 2 gives the resulting comparison between the CMM measured thicknesses over the conical and cylindrical sections of the test component and the corresponding values obtained ultrasonically using these optimized elastic constants. Overall, the ultrasonic measurements conform with the CMM measured thicknesses to within 2% (disregarding the end points, where the CMM measurements are prone to error).

Table 1. Room Temperature elastic constants in GPa:

	HERMANN[4]	ALBERTS[5]	PRESENT WORK
C_{11} (GPa)	251	248	258
C_{12} (GPa)	159	155	159
C_{44} (GPa)	132	132	129
$A = \frac{2C_{44}}{C_{11} - C_{12}}$	2.870	2.839	2.606
$C_{12}+2C_{44}$ (GPa)	423	419	417

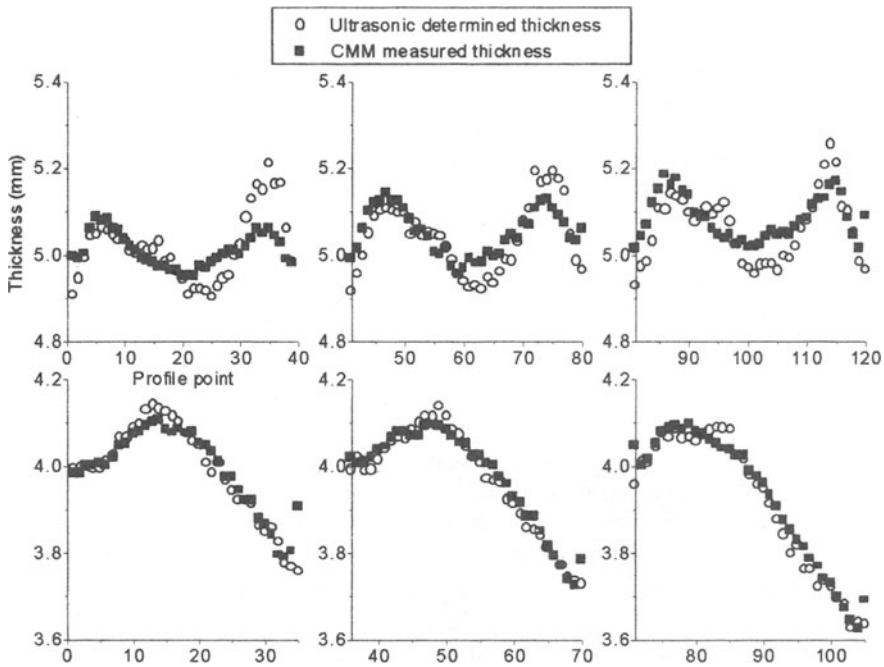

Figure 2: Thickness comparison on the test component for the cylindrical (upper diagrams) and conical sections (lower diagrams) respectively.

Similar measurements to above have been conducted on a turbine blade. Figure 3 shows a picture of the turbine blade. The six rod-like projections shown are surface-normal vectors generated by the blade's computer aided design (CAD) model.

The blade was scanned on the high and low pressure sides at 4 heights above the platform section, each scan being defined by 20 points. Afterwards the blade was sectioned so as to allow measurement of the actual thicknesses with the CMM. Figure 4 depicts one of those cross-sections of the turbine blade.

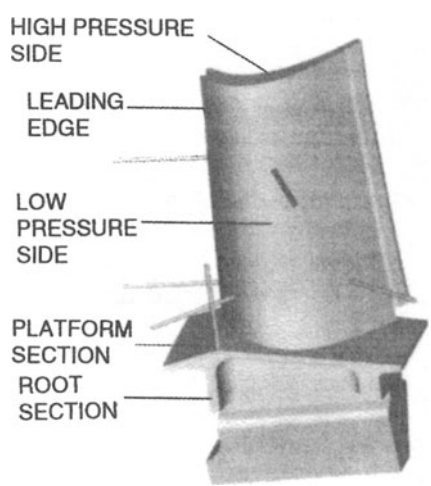

Figure 3: The jet engine turbine blade

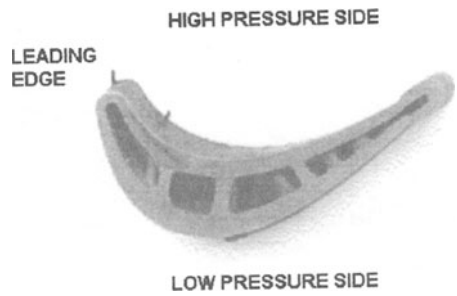

Figure 4: One of the cross-sectional views of the turbine blade.

Figure 5 shows in plan view the thickness comparison for one of the cross-sections. Shown are the external profile as measured by the CMM (dots), the internal profile as measured by the CMM (spline fit), and the internal profile as inferred from the ultrasonic data (dots). Approximately the same absolute accuracy was achieved on the turbine blade as with the testpiece, but because the wall thickness of the blade is about a factor of 4 smaller than that of the testpiece, the relative errors are larger for the blade, but nevertheless below 10%.

AMPLITUDE VARIATION OBSERVATION

There is considerable variation in the echo amplitudes for pulses propagating in different directions through our specimens. The main source of this variation, at least in the test component, is the acoustic anisotropy of the superalloy. This causes the transmission and reflection amplitudes at the front and back surfaces to be dependent on the surface orientation. A consequence of this is that well away from the high crystallographic symmetry directions there is significant mode conversion to T waves in the component. In some directions the T wave echoes thereby achieve a significant fraction of the L wave echo amplitude. A second and even more important affect of anisotropy is focusing brought about by the variable shape of the acoustic slowness or constant frequency surface. Because acoustic rays $\mathbf{V}=\nabla_{\mathbf{k}}\omega(\mathbf{k})$ are normal to this surface, the acoustic energy flux is inversely proportional to the Gaussian curvature K of the surface and hence, in the far field, there is a factor $\sqrt{(1/K)}$ in the echo amplitude that depends on direction. The variable wall thickness plays a somewhat smaller role in

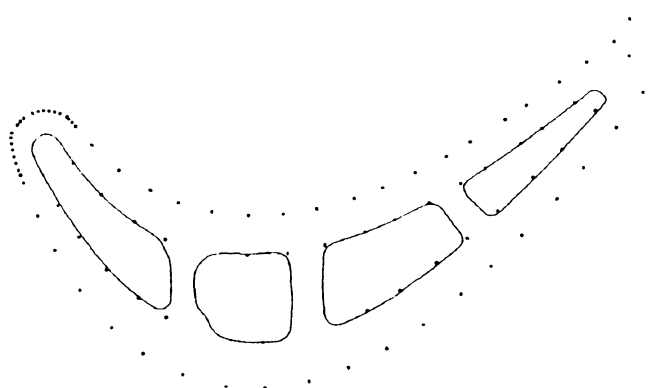

Figure 5: Comparison between the ultrasonic and measured thicknesses for one of the cross-sections of the turbine blade.

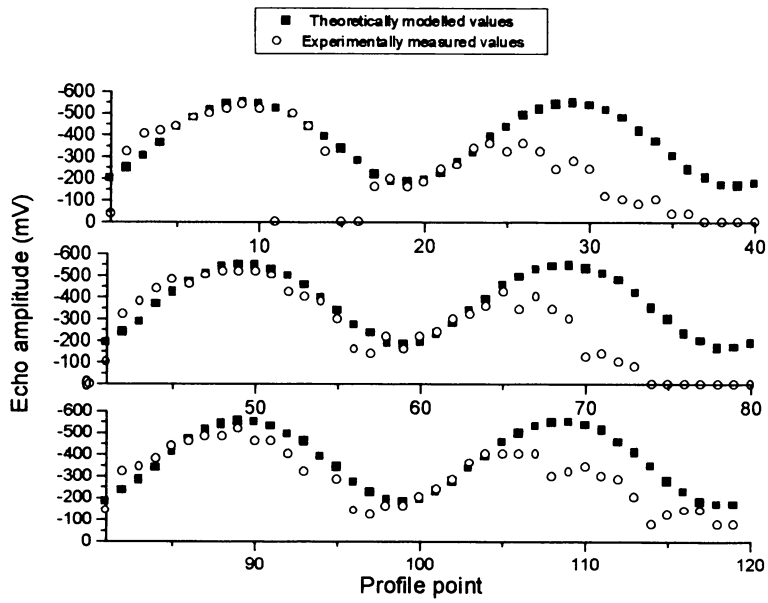

Figure 6: Backwall echo amplitude comparison at 3 different scan levels on the cylindrical section of the test component.

determining the echo amplitude. In the case of the turbine blade, the high curvature of the leading and trailing edges has a pronounced effect on the echo amplitudes, but we will not discuss that effect here.

The method we have implemented for calculating the directionally dependent echo amplitude is an extension of the approach of Levin[6]. It is based on the angular spectrum method for the acoustic field generated by the small aperture (half angle of the focal cone (θ_0=5.6) focused probe. We take into account all the mode conversion channels at the front and back surfaces and calculate for all the 9 possible mode sequences for a single passage of the wave back and forth through the specimen. For each mode sequence the progress of the wave field is followed through the specimen and the stationary phase approximation is invoked in the integration over the aperture to obtain the returning echo amplitude. The echo delay time is found to conform with Eq.(1) even though the path of the wave is in general oblique to the surface normal and in the direction of the ray vector. With the lens focus located on the front surface, the echo signal amplitude for each surface orientation is found to depend inversely on the square root of the Gaussian curvature at the corresponding point of the slowness surface of the superalloy. From observation and calculation the longitudinal mode echo is the dominant one in all directions, but varies considerably in amplitude as the probe is moved round the component. Figure 6 shows the amplitude variation of this echo at three different scanned heights as a function of profile point number. The measured data was obtained from the backwall echo amplitude using a stop threshold to obtain the negative voltage at the peaks. The main contributory factor in the *L* echo variation is the marked variation in the curvature of the *L* sheet of the slowness surface, while mode conversion plays a smaller role. For this reason the *L* mode amplitude is a minimum near the [100] crystallographic directions. The deviation of the last approximately 16 experimental points of each scan is a consequence of a slight change in crystallographic orientation at a small angle grain boundary near the middle of the component. The behavior of the *T* echo amplitudes is

more complex, being influenced by large variations in the mode conversion coefficients and also focusing. Our calculations are able to qualitatively explain this behavior.

CONCLUSION

Wall thickness measurements have been carried out on two single crystal nickel-based superalloy components, a specially cast testpiece and a gas turbine blade. The measurements on the testpiece yielded an optimized set of elastic constants for the superalloy. Mechanically and ultrasonically measured thicknesses agree to within 2% for the testpiece and 10% for the blade. Echo amplitude variations observed are in reasonable accordance with calculation. The simple analysis of the pulse transit time based on the phase velocity breaks down at the leading and trailing edges of the blade where the curvature is largest. A more detailed analysis taking into account this curvature is underway.

ACKNOWLEDGMENT

This paper was prepared with the support and facilities of the Materials Technology (MATTEK) division of the Council for Scientific and Industrial Research (CSIR) in Pretoria, South Africa.

REFERENCES

1. V. F. Muzhitskii, Yu. S. Kalinin and A. S. Sidorenko, *A computerized eddy-current system for monitoring the wall thickness of turbine blades made of heat-resistant alloys*, Russian Journal of Nondestructive Testing, 32 (1996), pps. 383-389.

2. R. A. Kline, J. B. Deaton, D. R. Howard, *Simultaneous determination of orientation and thickness in anisotropy media*, Review of Progress in Quantitative NDE, Vol. 16, Ed. D. O. Thompson and D. E. Chimenti, Plenum, NY (1997).

3. A. G. Every, *General closed form expressions for acoustic waves in elastically anisotropic solids*. Phys. Rev. B22 (1980), pps. 1746-1760.

4. W. Hermann, personal communication.

5. V. Alberts, personal communication.

6. V. Levin, *Advances in study of large-scale microstructure of real crystals using methods of acoustic microscopy*, Acoustical Imaging, Vol. 20, Ed. Y. Wei and B. Gu, Plenum, NY (1993), pps. 233-240.